Asian Journal of Chemistry; Vol. 37, No. 10 (2025), 2379-2386
ASIAN JOURNAL OF CHEMISTRY
https://doi.org/10.14233/ajchem.2025.33307

Enhanced Dielectric and Electromagnetic Interference Shielding Properties of Ag-PANI/BC Ternary Nanocomposites at Room Temperature

K.R. HEMANTHA KUMAR[1], M. REVANASIDDAPPA[2] and V. SRINIVASA MURTHY[1,*]

[1]Department of Chemistry, School of Engineering, Dayananda Sagar University, Bangalore-562112, India
[2]Department of Chemistry, PES University, Electronic City Campus, Bangalore-560100, India

*Corresponding author: E-mail: vsmurthy-chem@dsu.edu.in

Received: 31 December 2024 *Accepted*: 25 August 2025 *Published online*: 30 September 2025 AJC-22120

In this work, green tea extract and banana peels, natural ingredients, were used in the synthesis of silver-PANI/banana carbon (Ag-PANI/BC) ternary composites. *In situ* chemical polymerization method was adopted with incorporating varied weight percentage composition of banana peel derived carbon. The formation of the composite was confirmed by FTIR spectroscopic analysis, where the characteristic vibrational frequency bands confirmed the successful interaction and integration within the 8 wt.% Ag-PANI/BC ternary composite. The amorphous nature of PANI and Ag–PANI, as well as the semicrystalline structure of the Ag–PANI/BC ternary composite, were confirmed through powder X-ray diffraction (pXRD) analysis. Surface morphology observed from SEM images of the Ag–PANI/BC (8 wt.%) composite revealed granular, non-uniform, spherical-like structures with inhomogeneous surfaces, ranging in size from approximately 90 to 175 nm. The composite shown comparable AC conductivity 10^{-6} to 10^{-4} S/cm for 6, 8, & 10 wt.% composites measured in the frequency range 20 Hz to 10 MHz. The dielectric constant and tangent loss measurements indicate that the ternary composites are the promising candidates for energy storage applications operating at a frequency of 1000 Hz. Significantly, the 6 wt.% and 8 wt.% Ag–PANI/BC composites exhibited excellent electromagnetic interference (EMI) shielding effectiveness, achieving values of approximately 25-26 dB in the S-band (2.1-3.0 GHz), demonstrating their suitability for practical applications in electronic and electrical devices operating within this frequency range.

Keywords: Ag-polyaniline, Banana carbon, Electromagnetic interference, Shielding effectiveness, S-Band.

INTRODUCTION

Conducting polymers have seen fascinating technological applications in the field of electronics and electrical appliances as they can easily combine their chemical and mechanical properties with the electrical properties of metals and semiconducting materials [1,2]. Polyaniline (PANI) is found to be very useful conducting polymer in the field of academic as well as industrial research, due to its easy synthesis, processibility, economic viability and environmental stability [3]. Further, chemical stability and mechanical strength were found *via* synergistic effects when these conducting polymer materials are mixed with metals, metal oxides, organic compounds, non-metals and other polymers which were prepared by physical mixing/blending, chemical processes and other electrochemical pathways [4]. Interestingly, upon embedding PANI with silver nanoparticles, it has exhibited a remarkably enhanced electrical and electronic properties [5]. In addition, Ag-PANI composite has shown effective application as antibacterial agent and synergetic effectiveness over traditional antibiotic reagents in the broad range of pathogenic bacteria [6].

Recent advancements in the nanocomposite design have seen the integration of PANI with carbon nanotubes, graphene derivatives (including graphene oxide) and emerging 2D materials. Among these, transition metal dichalcogenides (TMDs) like WS_2 [7] and MoS_2 have gained attention for their multifunctionality in fields such as optoelectronics, CO_2 capture and reduction, hydrogen evolution reactions (HER), and gas sensing technologies [8,9]. Among the diverse applications of these intrinsically conductive polymer composites, the electromagnetic interference (EMI) shielding has emerged as one of the most promising areas of application for such materials [10]. EMI shielding effectiveness within the S-band (2–4 GHz) is particularly significant, given its relevance to the telecommunication sector, wireless sensors, Internet of

Things (IoT) devices, aerospace and defense technologies, medical devices, wearable electronics and automotive systems [11,12].

Recent studies have highlighted the promising applications of carbon-based elements integrated with conducting polymers [10]. As a fundamental and omnipresent element, carbon exhibits multiple allotropes such as graphene, carbon nanotubes and amorphous carbon, which enable a wide range of structural and functional tunability [13]. Increasingly, composite material research is aligning with green technology initiatives, focusing on the use of renewable and waste-derived resources. These efforts contribute to sustainable development while advancing the performance of such materials in the electronic and optoelectronic applications [14].

Further, to enhance the scope of the ternary composites of conducting polymers, we have chosen Ag-PANI composite with the carbon derived from the banana peel. As banana peel is rich in organic components such as starch, lignin, cellulose, proteins, pectin, *etc*. and its effectiveness as an adsorbent for organic and inorganic pollutants is attributed to the presence of diverse functional groups, internal microporosity and a high surface-to-volume ratio [15]. In literature, polypyrrole-banana carbon composite prepared *via* green chemistry approach has shown an excellent corrosion resistance and effective electromagnetic shielding properties [10]. Hence, considering the remarkable properties of the developed binary and ternary composites, this study investigates their AC conductivity and EMI shielding effectiveness. The ternary composites were synthesized through an *in situ* chemical polymerization process, employing green chemistry methods to extract both silver and carbon materials. The obtained ternary composite with varying wt.% of banana carbon were characterized with XRD, FT-IR and FESEM techniques. AC conductivity measurements and EMI shielding properties of the composites were also studied to explore their pertinent practical applicability for electrical and electronic devices.

EXPERIMENTAL

Aniline ($C_6H_5NH_2$) and hydrochloric acid were procured from S.D. Fine Chemicals, India. Ammonium persulphate was procured from Sigma-Aldrich, India. Aniline was double distilled prior to synthesis of the ternary composites. Throughout the synthesis of PANI and Ag-PANI/BC composites, distilled water was used. Carbon was prepared by drying banana peels at ambient temperature (~300 K), then cutting them into smaller pieces. These pieces were carbonized on an iron pan covered with a lid to obtain a blackish powder, which was finally ground into a fine powder using a pestle and mortar for further composite synthesis.

Preparation of Ag-PANI-BC ternary composites: Composites were prepared using 2 M aniline dissolved in 2 N HCl in a beaker then 0.1 M of $(NH_4)_2S_2O_8$ with green tea extract and $AgNO_3$ solutions were added separately dropwise along the sides of the beaker. Then known amount of BC (2%, 4%, 6%, 8% and 10%) in to the above solution in a controlled flow to start oxidation reaction under cooling. Obtained product after the *in situ* polymerization was allowed to dry in an oven at 60 ºC until to reach a constant weight and then powdered using a pestle-mortar. For EMI shielding measurements, the composites were mixed with known concentration of aqueous PVA solution to prepare the substrate-free films of the said composites as shown in Fig. 1.

Characterization: Fourier-transform infrared spectroscopic data was obtained using Nicolet 750 FTIR instrument in the frequency range 4000-250 cm^{-1}. Surface morphology of the composite was analyzed with the assistance of scanning electron microscope (SEM) of make A Zeiss Ultra 60 instrument by loading the samples on an aluminium tape. Also, an elemental composition was determined by energy dispersive X ray spectroscopy (EDX). XRD spectra of PANI, BC and Ag-PANI-BC (10%) composite were performed in the range $2\theta = 10^o$ to 80^o by Siemens D-5000 powder X-ray diffractometer (Germany) with Cu*K*α radiation (λ = 1.54 Å).

AC conductivity measurements: Before measuring AC conductivity, the samples were processed with the help of pestle and mortar to get fine granular powder. Silver doped PANI pellet and Ag-PANI/BC composite pellets were obtained with measuring diameter of 13.4 mm and thickness of 1.4 mm by applying approximately 5-ton pressure in a hydraulic pressing machine. AC readings were collected with the frequency range 20-10 MHz. Instrument of make LCR meter (Japan) Hioki model 3532-50 connected with programmable computer.

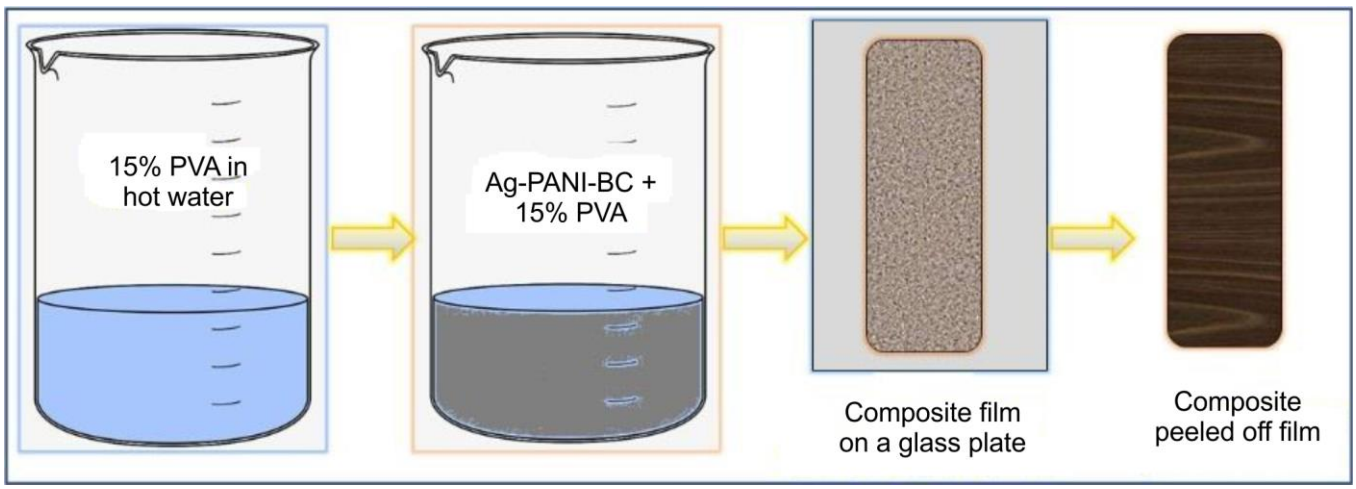

Fig. 1. Preparation of Ag-PANI/BC composites thin films for EMI-SE measurements

EMI shielding measurements: EMI shielding effectiveness (EMI SE) of BC composites Ag-PANI/BC (6%) and Ag-PANI/BC (8%) were measured in a frequency range 2-3 GHz (S-band) using the lab fabricated experimental set up. The input of the waveguide was supplied by a RIGOL signal generator and the output was directed to a Tektronix spectrum analyzer for measurement of the residual frequency. This frequency was recorded through a computer interfaced data recorder.

EMI shielding effectiveness (in dB) of the sample can be measured by logarithmic ratio of input power to the out power of the signal. Mathematically, EMI shielding effectiveness is a negative quantity as the out power is always less than the input power. When a microwave radiation is incident at the shield reflection, absorption and transmission of the signal occurs. Hence, the effectiveness of the shield is logically due to the reflection and the absorption parts, which can be expressed as follows (eqn. 1) [16]:

$$SE_t = SE_r + SE_a = 10\log\left(\frac{P_t}{P_i}\right) \quad (1)$$

RESULTS AND DISCUSSION

FTIR studies: Fig. 2a presents the FTIR absorption spectrum of PANI, where the distinctive band at 1135 cm^{-1} corresponds to C–N *tertiary* aromatic vibrations. The band observed at 1301 cm^{-1} corresponds to C–N primary and secondary vibrations [17], while the broad band between 3450 and 3200 cm^{-1} is attributed to N–H stretching vibrations. The bands at 1567 and 1478 cm^{-1} are assigned to the quinoid and benzenoid structures, respectively, with the band at 1242 cm^{-1} corresponding to the C–N stretching mode of the benzenoid ring. The *para* substituted aromatic ring vibrations at 810 cm^{-1} can be attributed to the out-of-plane bending vibrations. The above frequency bands are in par with the earlier reported values [18]. Fig. 2b depicts IR absorption spectrum of Ag-PANI, in which absorption peak around 1305 cm^{-1} is attributed to the polaronic structure of PANI. The band at 1245 cm^{-1}, assigned to the protonated chain vibration of PANI, shifts to 1230 cm^{-1} upon doping with silver particles. This shift is attributed to the reduction of Ag^+ to Ag^0 and the simultaneous oxidation of the amine (–NH–) groups in the PANI backbone to imine (–N=) groups [19]. The additional bands at 494 and 422 cm^{-1} are due to presence of silver in the composite [20]. Fig. 2c depicts the FTIR spectrum of bacterial cellulose (BC), showing a band at 1125 cm^{-1} corresponding to C–C absorption and a band at 1645 cm^{-1} attributed to C=C stretching vibrations, suggesting the presence of other carbon allotropes. Fig. 2d displays the FTIR spectrum of the ternary composite, where the characteristic absorption band at 3213 cm^{-1} indicates N–H stretching vibrations of PANI, while the band at 1645 cm^{-1} exhibits a minor variation in intensity, confirming the incorporation of BC within the composite.

XRD studies: XRD spectrum of PANI, Ag-PANI, BC and Ag-PANI/BC composites are shown in Fig. 3. Fig. 3a depicts the X ray diffraction (XRD) pattern of PANI, clearly evidences two broad peaks at 2θ = 21.3º and the unique peak at 25.5º can be attributed to the lattice periodicity in the direction along the PANI chains and normal to the polymer chains [18]. These two peaks of PANI representing the short range of chain ordering. Fig. 3b bear diffraction pattern of Ag-PANI providing the Bragg reflections at 2θ = 19.2º and 26.1º are attributed to organization of periodicities along the backbone chain of PANI and orthogonal to the polymer chains, respectively. "The additional diffraction peaks observed at 2θ =

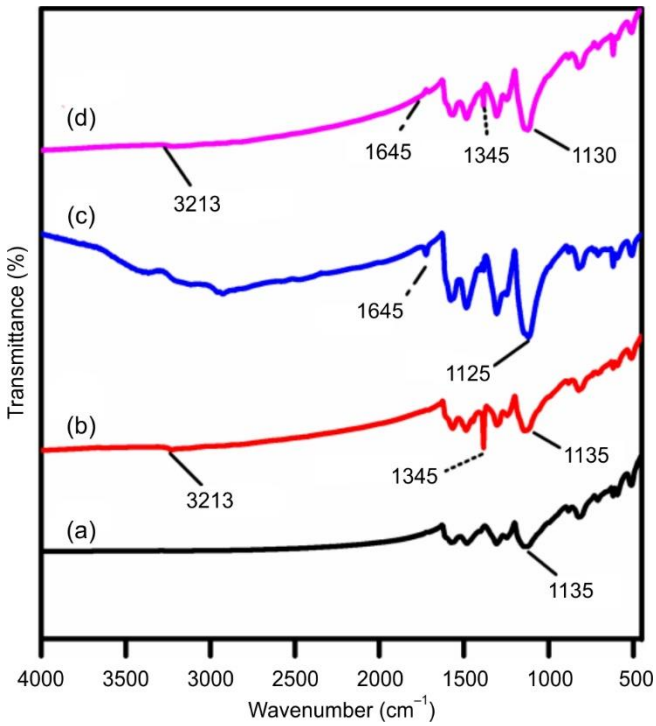

Fig. 2. FTIR spectra of (a) PANI, (b) Ag-PANI, (c) BC and (d) Ag-PANI/BC (8%) composites

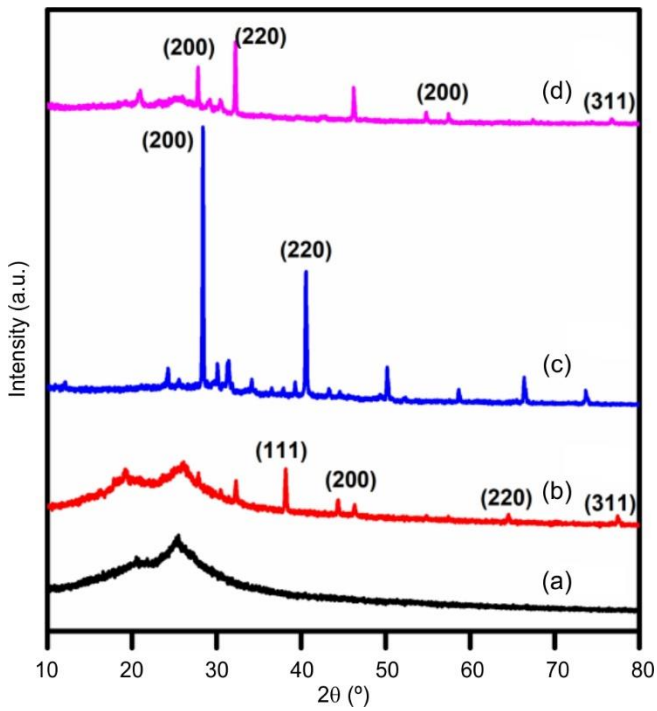

Fig. 3. XRD patterns of (a) PANI, (b) Ag-PANI, (c) BC and (d) Ag-PANI/BC (8%)

38.1º, 44.3º, and 64.5º correspond to the (111), (200), and (220) Bragg reflection planes, respectively, characteristic of the face-centered cubic (fcc) structure of silver. These silver peaks exhibit relatively lower intensity compared to the diffraction peaks associated with the PANI chains [19]. The XRD pattern of the synthesized bacterial cellulose (Fig. 3c) matches the JCPDS card No. 00-041-1476, corresponding to KCl with a cubic space group ($Pm\bar{3}m$), confirming its crystalline nature. XRD of the BC shows characteristic peaks at 2θ = 28.3º related to (200) and 40.6º corresponding to (220) planes [14]. Also, a small peak at 2θ = 24.2º corresponds to carbon peak of (002) plane, indicating the presence of amorphous carbon in the BC sample. XRD of Ag-PANI/BC composites (Fig. 3d) displayed the sharp peaks at 2θ = 29º, which showed the incorporation of BC in the composite. Characteristic peaks corresponding to Ag-PANI and BC is evidenced in Ag-PANI/BC composite, which clearly reveals the formation of the composite. The peaks corresponding to banana carbon (BC) observed in the composite exhibit reduced intensity, indicating its retained crystalline nature and confirming the successful incorporation of BC into the Ag-PANI polymer matrix. Notably, an increase in the weight percentage of BC within the composite correlates with the enhanced crystallinity, further supporting the formation of crystalline ternary composites.

Morphological studies: Fig. 4 shows the SEM and EDX images of the sample. In Fig. 4a, one can see the uniform distribution of granular structures of PANI with average size in the 100-500 nm range [20]. Fig. 4b shows Ag-PANI particles also can be observed in granular structures of comparatively smaller average sizes around 50 to 300 nm. Fig. 4c represents the morphological features of BC, wherein flakes like structures with uneven surfaces of sizes in the range 200-800 nm were observed. Fig. 4d shows the morphology of the Ag-PANI/BC (8%) composite, revealing granular, non-uniform spherical-like structures with irregular surfaces, ranging in size from 90 to 175 nm. Incorporation of BC in the composite is evident from this surface morphology data, wherein decreased size of BC, favours ion enhancing surface area contributing to increased charge transfer yielding higher conductivity.

Fig. 4e shows energy dispersive X-ray spectrum (EDX), revealing the peaks of carbon, nitrogen and chloride of the Ag-PANI/BC composite in the suitable proportion. These peaks confirm the successful formation of the composite and the elemental composition of Ag-PANI/BC (8%) was found to be consistent with the intended proportions used during synthesis.

AC conductivity studies: AC conductivity in disordered materials can be obtained with the help of equation [$\sigma(f) = \sigma'(f) - i\,\sigma''(f)$], where $\sigma'(f)$ is for real part and $\sigma''(f)$ constitutes the imaginary conductivity of the composites. General behaviour of the real part of conductivity $\sigma'(f)$ in disordered materials takes the form. Measured AC conductivity results are shown in Fig. 5. AC conductivity measurements with varied frequency from 20 Hz to 10 MHz. The composites with 2% to 6% and 10% filler content exhibited a gradual plateau increase in conductivity with increasing frequency. This behaviour is likely due to a lower surface charge density, which is suppressed by the carbon present in the ternary composite. The significant conductive behaviour observed can be attributed to the presence of Ag and PANI, consistent with the conductivity values reported for pure PANI and Ag-PANI composites. In addition, carbon is neither creating charge

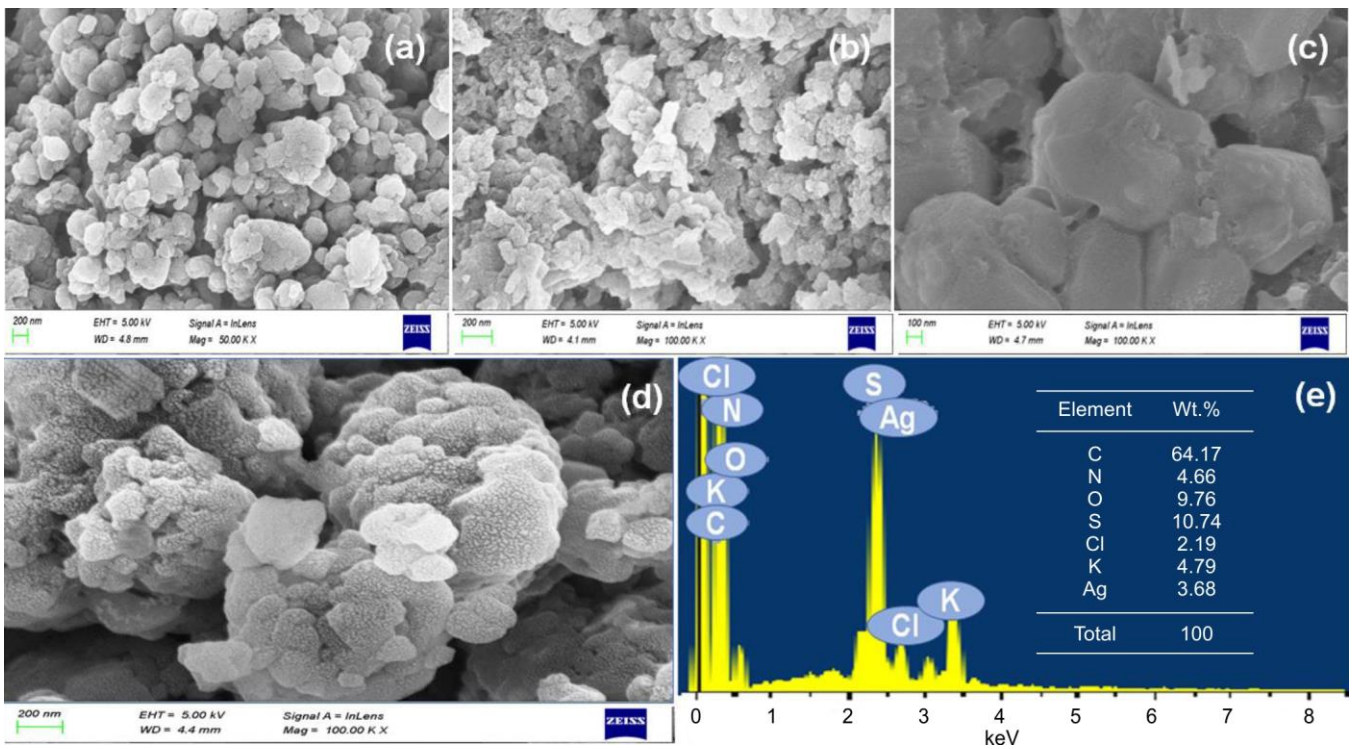

Fig. 4. Scanning electron micrographs of (a) PANI, (b) Ag-PANI, (c) BC and (d) Ag-PANI/BC (8%) and (e) EDX spectrum of Ag-PANI/BC (8%)

carriers nor pocesses conjugation essential for conducting behaviour of the composite. The lack of significant surface charge carriers in the BC-doped composites suggests that no polaron hopping frequency is observed. The polarons and bipolarons present are primarily derived from PANI, as evidenced by the minimal variation in conductivity values between the PANI/Ag-PANI and BC-containing composites. For transfer of the charges, applied frequency is insufficient to surpass the insulating behaviour of carbon. Increasing frequency enhances ion movement and surface charge carrier capacity, improving conduction. However, variations in the carbon allotropes dependent on the synthetic method and also concentration may contribute to the lower conductivity of Ag-PANI/BC composites. Conductivity plots indicate that BC is unevenly distributed within the PANI/Ag-PANI matrix, disrupting the conduction network and weakening polymer–BC interactions, which results in reduced carrier mobility and lower electrical conductivity.

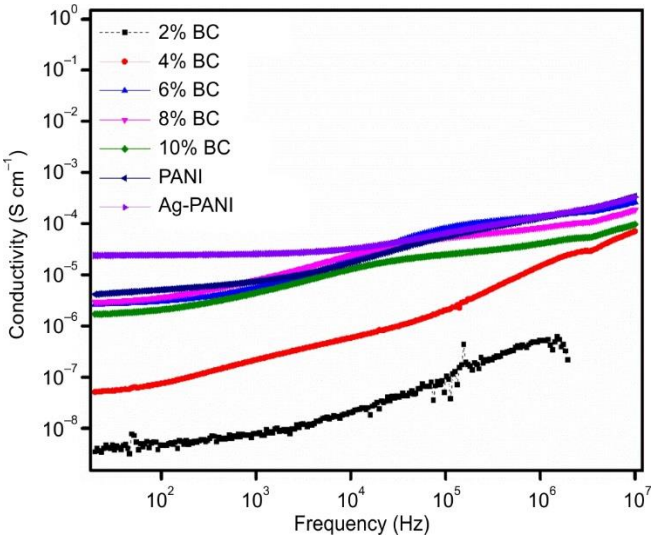

Fig. 5. AC conductivity measurements with variation of applied frequency

Dielectric constant and tangent loss were calculated as a function of frequency for all the varied% of BC in the prepared composites. Fig. 6 demonstrates the change in dielectric constant as a function of applied AC frequencies for Ag-PANI/BC composites. Across the applied AC frequencies, dielectric constant was found to be in the order of 10^4 at lower frequency for composites of concentration 4%, 6% and 10%, the value is found to decreases MHz. On the other hand, 8% composite has shown 10^3 at 20 Hz and exhibits very slow decrease up to 10^2 at 10 MHz frequency. This linear fashion of decreasing dielectric constant gradually, demonstrating the characteristic dielectric properties of the conducting polymer composites, which is on resemblance with recent studies reported [21]. Greater the permittivity values at lower frequencies may be the attributing factor for electrode polarization and space charge polarization effects [22]. Decrease in the dielectric constant as frequency increases can be explained by Maxwell-Wagner polarization model [23]. Variation in the dielectric constant with the applied frequencies can be explained on the base of hopping frequency of the charge carriers. Since, the hopping frequency of the charge carriers

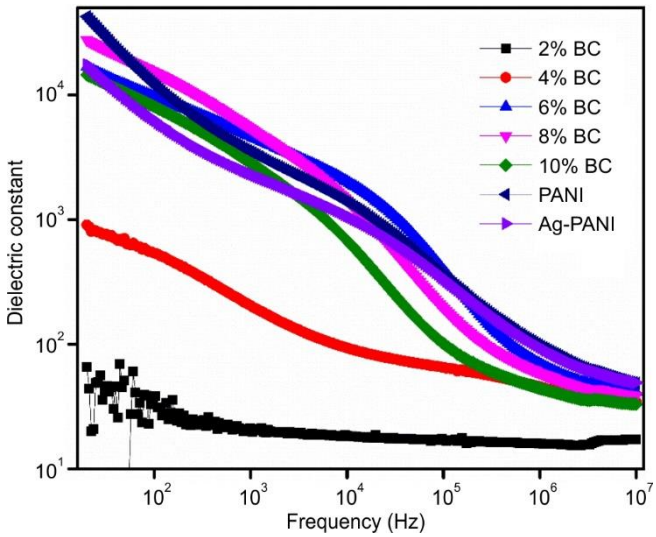

Fig. 6. Variation of dielectric constant as a function of applied frequency for 2, 4, 6, 8 and 10% Ag-PANI/BC composites

follows frequency of the applied field, which marks in higher values of dielectric constant. In contrast, at higher frequencies, hopping frequency lags the applied frequency of the AC field, which results in the dielectric constant of lower values due to the random dipolar orientation [24]. At 1000 Hz frequency 6 and 8 wt.% composites have shown greater dielectric constant of around 4700 to 5500, which suggests that the prepared composites are superior for the storage devices like supercapacitor operating in this frequency range. Noticeably, 2% composite shown anomalous behaviour over other and plateau values across all the frequency range under the study.

The variation of the loss tangent (tan δ) with increasing applied frequency for the composites is shown in Fig. 7. All composites exhibit anomalous dielectric behaviour characterized by dielectric relaxation peaks. These relaxation phenomena can be explained using the Rezlescu model [25]. Moreover, this distinctive dielectric response is attributed to the hopping of small polarons, which significantly contribute to charge polarization [26]. The dielectric relaxation peaks arise when the hopping frequency of localized charge carriers resonates with the externally applied AC frequency [27]. Furthermore, the loss tangent (tan δ) values are higher at lower frequencies, indicating the presence of relaxation peaks. Except for the 2% composite, all other samples exhibit a linear decreesing trend in tan δ with increasing frequency. The 2% composite shows anomalous behaviour around 20 Hz, followed by a more rapid decline as the frequency increases. Elevated tan δ values at low frequencies may be advantageous for the design of medium-frequency devices. At 1000 Hz, the loss tangent is approximately 10, indicating minimal energy dissipation and suggesting suitability for energy storage applications. These findings are consistent with the dielectric constant measurements, collectively highlighting the promising potential of the 6 wt.% and 8 wt.% composites for such applications.

Therefore, the observed decrease in dielectric constant and conductivity with increasing frequency indicates that the higher dielectric constant values are primarily due to the conduction relaxation as discussed earlier. The high dielectric

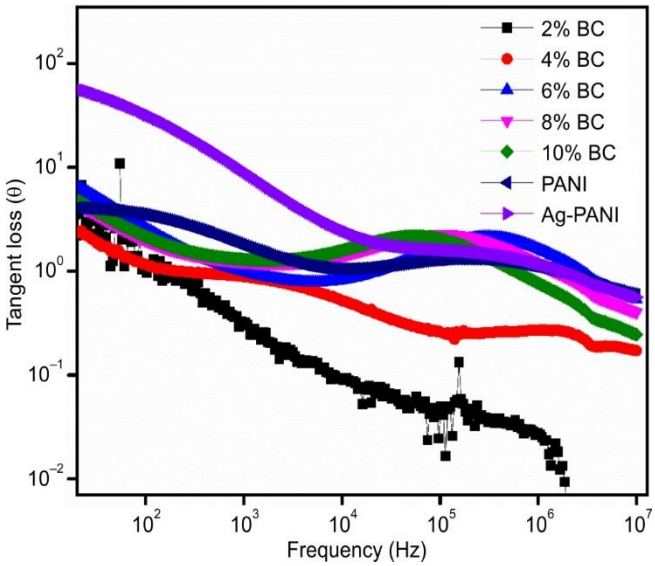

Fig. 7. Variation of tan θ as a function of frequency for Ag-PANI/BC composites with different concentration of BC of 2, 4, 6, 8 and 10%

loss at lower frequencies in all composites can be attributed to losses caused by DC conduction. These results align with the trends noted for decreasing doping levels, thereby providing further insight into the dielectric behaviour of the materials.

Fig. 8 presents the variation of the real part of the dielectric modulus (M′) as a function of the logarithm of frequency, revealing two distinct segments in the composite system. The first segment corresponds to 2 and 4% composites show flattened pattern ascribing to very narrow variation in the M′ values at applied frequency range, suggesting that the polarization of the electrode to M′ make a constant contribution to the nanocomposite materials. In the second segment, corresponding to the 6%, 8% and 10% composites (M′) exhibits a linear increase with applied frequency. This behaviour can be attributed to conduction phenomena associated with the short-range mobility of charge carriers, particularly ions.

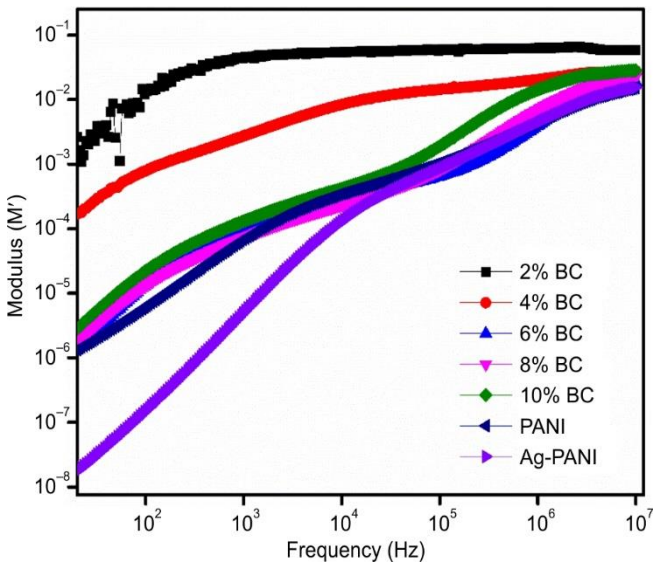

Fig. 8. Real dielectric modulus M′ of 2, 4, 6, 8 and 10% Ag-PANI/BC composites as a function of applied frequency in the range from 20 Hz to 10 MHz

Electrical modulus behaviour, the complex permittivity (ε″) related to the electrical modulus (M′ and M″) is given as below [28-31]:

$$M^* = M' + M'' \quad (1)$$

$$M' = \frac{\varepsilon'}{\varepsilon'^2 + \varepsilon''^2} \quad (2)$$

$$M'' = \frac{\varepsilon''}{\varepsilon'^2 + \varepsilon''^2} \quad (3)$$

Fig. 9 shows the values for the imaginary part (M″) of the electrical modulus with variation of F. The lower values of the imaginary part (M″) for 6,8 and 10% composite at the lower frequency are the sign of transport of the ions. Distinct relaxation peaks observed in the curves are attributed to the structural imperfections within the crystalline phase. Moreover, the increasing peak intensity of M″ with frequency suggests that boundary contributions significantly influence the relaxation mechanism. In contrast, other two composites 2 and 4% are contradictory to observation obtained for 6, 8 and 10%.

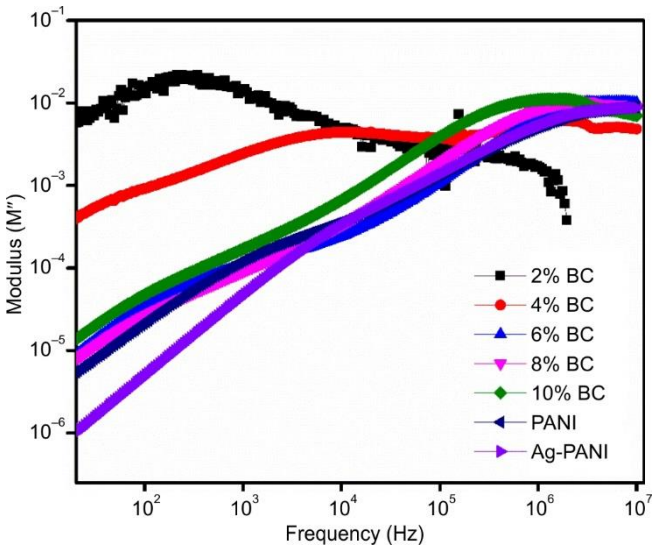

Fig. 9. Imaginary dielectric modulus M″ of 2, 4, 6, 8 and 10% Ag-PANI/BC composites as a function of applied frequency in the range from 20 Hz to 10 MHz

EMI shielding effectiveness: It is well-known from reported literature, with the basis of EMI shielding theory (SE) is directly proportional to electrical properties of the nanocomposites [32]. Ag-PANI/BC composites with 6% and 8% filler content exhibited superior dielectric properties and demonstrated effective EMI shielding with values of approximately 25 and 26 dB, respectively, in the 2.1–3.0 GHz (S-band) frequency range, as shown in Fig. 10. This kind of EMI SE is useful for the protection of the electronic gadgets working in S-band as reported in earlier literature [33].

The shielding mechanism in polyaniline (PANI) is primarily attributed to the orientational polarization and space charge polarization. Intrinsic conducting polymers such as PANI possess conjugated double bonds along their polymer chains. These conjugated polymers contain both free and bound charges that contribute to their transport properties.

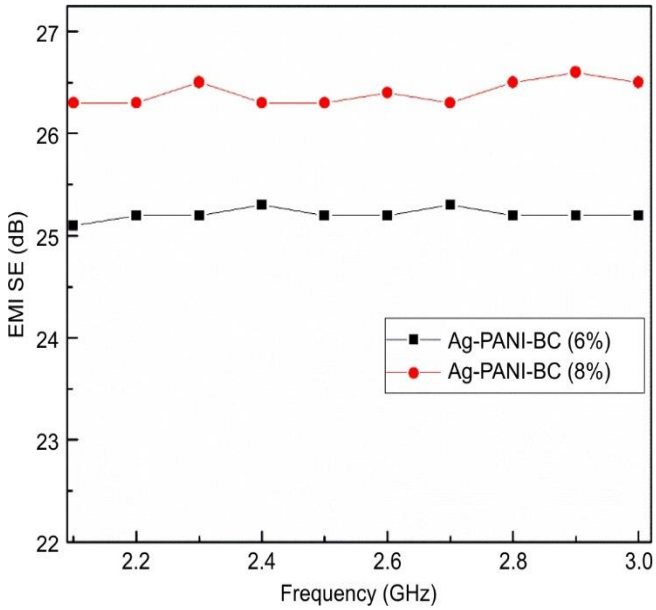

Fig. 10. Frequency *versus* EMI SE Ag-PANI/BC composites of 6% and 8%

Free charges, represented by polarons and bipolarons, move along the polymer chains, while bound charges correspond to dipoles with limited mobility, resulting in strong polarization [34]. Similar charge transfer mechanisms are observed in Ag-decorated PANI composites with carbon derived from banana peel. Specifically, Ag-PANI-BC composites with 6% and 8% filler content demonstrate effective electromagnetic interference (EMI) shielding, primarily due to space-charge polarization effects analogous to those in pure PANI [10].

Conclusion

Ag-PANI/BC composites were prepared using *in situ* polymerization method. In the prepared composites, the fillers Ag and carbon from banana peel (BC) were successfully extracted using green chemistry approach. FTIR studies support the incorporation of BC in the ternary composite. The X-ray diffraction pattern confirms the retention of the crystalline nature of banana peel carbon (BC) and its well-integrated interface within the Ag-PANI polymer matrix. SEM analysis further supports the uniform dispersion of BC in the nanocomposite, while EDX analysis verifies the presence of carbon derived from banana peel. Conductivity measurements demonstrate enhanced electrical performance, with 2% and 4% composites showing a linear increase in AC conductivity with frequency, whereas 6%, 8%, and 10% composites exhibit frequency-independent, higher conductivity values comparable to Ag-PANI, indicating effective filler concentration. Although BC addition does not significantly enhance conductivity in the ternary composites, these materials remain suitable for electrical insulation applications. The dielectric constant and loss tangent values suggest potential for energy storage devices such as supercapacitors. Furthermore, EMI shielding effectiveness of approximately 26 dB in the S-band correlates well with conductivity results, highlighting the composites' suitability for shielding applications. Future work will explore performance in higher frequency bands, including C-, X-, and Ku-bands, for broader technological relevance.

ACKNOWLEDGEMENTS

The authors are thankful to the Management of PES University, Bangalore and Vision Group on Science and Technology, to support to carry out this research work, PESUIRF/Chemistry-ECC/2020/14 dated 30-09-2020. One of the authors, K.R. Hemantha Kumar, acknowledges to Syngene International Limited for providing the permission to do the research.

CONFLICT OF INTEREST

The authors declare that there is no conflict of interests regarding the publication of this article.

REFERENCES

1. H.M. Rashmi, M. Revanasiddappa, S. Manjunatha, M. Surekha and Y.T. Ravikiran, *Chem. Pap.*, **78**, 1435 (2023); https://doi.org/10.1007/s11696-023-03169-5
2. B.M.B.B. Patel, M. Revanasiddappa, D.R. Rangaswamy, S. Manjunatha and Y.T. Ravikiran, *Mater. Today Proc.*, **49**, 2253 (2022); https://doi.org/10.1016/j.matpr.2021.09.337
3. V. Babel and B.L. Hiran, *Polym. Compos.*, **42**, 3142 (2021); https://doi.org/10.1002/pc.26048
4. M. Beygisangchin, S. Abdul Rashid, S. Shafie, A.R. Sadrolhosseini and H.N. Lim, *Polymers*, **13**, 2003 (2021); https://doi.org/10.3390/polym13122003
5. K. Vinay, M. Revanasiddappa, S. Manjunatha, K. Shivakumar and Y.T. Ravikiran, *Mater. Res. Express*, **6**, 104003 (2019); https://doi.org/10.1088/2053-1591/ab3624
6. S.G. Mohammad, D.E. Abulyazied and S.M. Ahmed, *Desalination Water Treat.*, **170**, 199 (2019); https://doi.org/10.5004/dwt.2019.24694
7. S. Manjunatha, S. Rajesh, P. Vishnoi and C.N.R. Rao, *J. Mater. Res.*, **32**, 2984 (2017); https://doi.org/10.1557/jmr.2017.224
8. G.-J. Lai, L.-M. Lyu, Y.-S. Huang, G.-C. Lee, M.-P. Lu, T.-P. Perng, M.-Y. Lu, and L.-J. Chen, *Nano Energy*, **81**, 105608 (2021); https://doi.org/10.1016/j.nanoen.2020.105608
9. A. Sunilkumar, S. Manjunatha, T. Machappa, B. Chethan and Y.T. Ravikiran, *Bull. Mater. Sci.*, **42**, 271 (2019); https://doi.org/10.1007/s12034-019-1955-5
10. C.K. Madhusudhan, K. Mahendra, M. Revanasiddappa and M. Faisal, *J. Mater. Sci. Mater. Electron.*, **33**, 1366 (2022); https://doi.org/10.1007/s10854-021-07466-1
11. A. Sedighi, R.A. Taheri and M. Montazer, *Ind. Eng. Chem. Res.*, **59**, 12774 (2020); https://doi.org/10.1021/acs.iecr.0c02141
12. N. Maruthi, M. Faisal and N. Raghavendra, *Synth. Met.*, **272**, 116664 (2021); https://doi.org/10.1016/j.synthmet.2020.116664
13. I.J. Gómez, M. Vázquez Sulleiro, D. Mantione and N. Alegret, *Polymers*, **13**, 745 (2021); https://doi.org/10.3390/polym13050745
14. L. Zheng, B. Sun, S. Mao, S. Zhu, P. Zheng, Y. Zhang, M. Lei and Y. Zhao, *ACS Appl. Bio Mater.*, **1**, 496 (2018); https://doi.org/10.1021/acsabm.8b00226
15. S.G. Mohammad, S.M. Ahmed, A.F.M. Badawi and D.S. El-Desouki, *J. Appl. Life Sci. Int.*, **3**, 77 (2015); https://doi.org/10.9734/JALSI/2015/16652
16. M. Mishra, A.P. Singh, V. Gupta, A. Chandra and S.K. Dhawan, *J. Alloys Compd.*, **688**, 399 (2016); https://doi.org/10.1016/j.jallcom.2016.07.190
17. S. Manjunatha, R. Megha, B. Chethan, M. Prashantkumar, Y.T. Ravikiran and T. Machappa, *J. Mater. Eng. Perform.*, **30**, 1885 (2021); https://doi.org/10.1007/s11665-021-05526-5
18. S. Manjunatha, T. Machappa, Y.T. Ravikiran, B. Chethan and A. Sunilkumar, *Physica B*, **561**, 170 (2019); https://doi.org/10.1016/j.physb.2019.02.063

19. B. Massoumi and S. Fathalipour, *Polym. Sci. Ser. A*, **56**, 373 (2014); https://doi.org/10.1134/S0965545X14030110
20. L.B. Gunjal, S. Manjunatha, B. Chethan, N.M. Nagabhushana, Y.T. Ravikiran, T. Machappa and S. Thomas, *MRS Commun.*, **13**, 248 (2023); https://doi.org/10.1557/s43579-023-00336-3
21. S. Manjunatha, T. Machappa, A. Sunilkumar and Y.T.T. Ravikiran, *J. Mater. Sci. Mater. Electron.*, **29**, 11581 (2018); https://doi.org/10.1007/s10854-018-9255-1
22. H.M. Kim, C.Y. Lee and J. Joo, *J. Korean Phys. Soc.*, **36**, 371 (2000).
23. Z. Yu and C. Ang, *J. Appl. Phys.*, **91**, 794 (2002); https://doi.org/10.1063/1.1421033
24. S. Sinha, S.K. Chatterjee, J. Ghosh and A.K. Meikap, *Polym. Compos.*, **38**, 287 (2017); https://doi.org/10.1002/pc.23586
25. J. Bao, J. Zhou, Z. Yue, L. Li and Z. Gui, *J. Magn. Magn. Mater.*, **250**, 131 (2002); https://doi.org/10.1016/S0304-8853(02)00364-5
26. I. Sadiq, S. Naseem, M.N. Ashiq, M.A. Khan, S. Niaz and M.U. Rana, *Prog. Nat. Sci.*, **25**, 419 (2015); https://doi.org/10.1016/j.pnsc.2015.09.011
27. V.R. Ramani, B.M. Ramani, A.D. Saparia, D. Dhruv and J.H. Markna, *J. Nano Res.*, **37**, 68 (2015); https://doi.org/10.4028/www.scientific.net/JNanoR.37.68
28. T.A. Hanafy, K. Elbanna, S. El-Sayed and A. Hassen, *J. Appl. Polym. Sci.*, **121**, 3306 (2011); https://doi.org/10.1002/app.33950
29. P. Maji, P.P. Pande and R.B. Choudhary, *Bull. Mater. Sci.*, **38**, 417 (2015); https://doi.org/10.1007/s12034-015-0886-z
30. N.S. Alghunaim, *J. Mater. Res. Technol.*, **8**, 3596 (2019); https://doi.org/10.1016/j.jmrt.2019.05.022
31. M. Rahaman, T.K. Chaki and D. Khastgir, *J. Mater. Sci.*, **46**, 3989 (2011); https://doi.org/10.1007/s10853-011-5326-x
32. A. Sunilkumar, S. Manjunatha, Y.T. Ravikiran, S. Thomas and T. Machappa, *Chem. Zvesti*, **77**, 4913 (2023); https://doi.org/10.1007/s11696-023-02828-x
33. L.L. Wang, B.K. Tay, K.Y. See, Z. Sun, L.K. Tan and D. Lua, *Carbon*, **47**, 1905 (2009); https://doi.org/10.1016/j.carbon.2009.03.033
34. C.K. Madhusudhan, K. Mahendra, B.S. Madhukar, T.E. Somesh and M. Faisal, *Polym. Sci. Ser. B*, **63**, 280 (2021); https://doi.org/10.1134/S156009042103009X